Influence of Förster-type energy transfer on the vibrational relaxation of anionic hydration shells

Stephan Lotze[a] and Huib J. Bakker
FOM Institute for Atomic and Molecular Physics, Science Park 104, 1098 XG Amsterdam, The Netherlands

(Received 3 April 2013; accepted 8 July 2013; published online XX XX XXXX)

We study the influence of Förster energy transfer on the vibrational relaxation dynamics of anionic hydration shells by performing time-resolved mid-infrared spectroscopy on the OH-stretch vibration of water molecules in aqueous solutions of sodium iodide. We observe that the Förster energy transfer leads to a pronounced acceleration of the vibrational relaxation. We describe the observed dynamics with a model in which we include the Förster vibrational energy transfer between the different hydroxyl groups in solution. With this model we can quantitatively describe the experimental data over a wide range of isotopic compositions and salt concentrations. Our results show that resonant energy transfer is an efficient mechanism assisting in the vibrational relaxation of anionic hydration shells.
 [http://dx.doi.org/10.1063/1.4816370]

I. INTRODUCTION

The introduction of ions into the hydrogen-bonding network of liquid water leads to a disruption of the tetrahedral hydrogen-bonding arrangement, as was first observed with linear absorption and Raman experiments.[1] An important question related to ions in water concerns the range over which ions influence the structure of aqueous salt solution. Based on viscosity measurements and thermodynamics properties, the influence of ions on the hydrogen bonding network of water has been discussed in terms of "structure makers" and "structure breakers," an idea that was first introduced in the 1930s by Cox and Wolfenden.[2] The term "structure makers" refers to small ions with a high charge density such as F^-, which are thought to have an ordering effect on the hydrogen bonding network, whereas "structure breakers" generally describes larger ions with a low charge density such as Cs^+ that presumably lead to a weakening of the overall hydrogen bonding strength of water.[3]

Over the past decade, time-resolved infrared spectroscopy has proven to be a useful technique to study the dynamics of water molecules both in the pure liquid and in the hydration shells of ions.[4–12] The hydroxyl stretch vibration (OH- or OD-stretch) has been the focus of most of the mid-infrared pump-probe-studies on aqueous salt solutions, since this mode forms a highly sensitive spectroscopic marker for the local environment of a water molecule.[4–14] These spectroscopic studies have yielded valuable information on the vibrational[8,9] and reorientational[5,7,11,12] dynamics of water and on the dynamics of its hydrogen bonding network.[7,10,14] For example, the reorientational motion and the spectral diffusion dynamics of water molecules residing in the hydration shell of halide anions have both been found to show a very slow component in comparison to the dynamics of pure water.[6,15,16] The lifetime of the hydroxyl stretch vibration has been found to vary substantially in different hydrogen bonding environments. Several studies on aqueous salt solutions have shown that the formation of a hydrogen bond to a halide ion leads to a substantial increase in the lifetime of the hydroxyl-stretch vibration.[7,8] Similarly, for water contained in AOT reverse micelles, it was observed that the water molecules forming weak hydrogen bonds to the sulfonate groups of the AOT surfactants, also show a significantly slower vibrational relaxation, with a T_1 time constant on the order of 3 ps.[17,18] The question of how long a water molecule resides in the hydration shell of an ion has been addressed by the groups of Fayer and Gaffney. In their studies, they observe a dynamical exchange between water molecules residing in anionic hydration shells and bulk water molecules that takes place on a time scale of 7 ps for BF_4^-[6] and 9 ps for ClO_4^-,[15] respectively. In both studies the rotation of water molecules out of the hydration shell was found to take place via large angular jumps. This mechanism of water reorientation has been predicted by Laage and Hynes.[16] The same mechanism is also active in bulk water.[19]

Nearly all of the previously mentioned time-resolved infrared experiments have been performed on either the OD-stretch vibration of HDO molecules dissolved in H_2O or the inverse system (OH-stretch of HDO in D_2O).[4–11,13,14,20–23] However, in real life, aqueous solutions usually contain pure H_2O, which has properties that are distinct from the aforementioned isotopic mixtures. One important feature of neat H_2O is the presence of efficient Förster resonant energy transfer between the OH-stretch vibrations. Förster resonant energy transfer has been studied both in neat H_2O and D_2O,[24–26] and has been found to lead to an ultrafast redistribution of the excitation energy over neighboring OH (OD)-groups. In isotopic solutions resonant energy transfer is suppressed because of the increase in average distance between OH groups.

In view of this work, it is interesting to see how Förster resonant energy transfer affects the vibrational dynamics of water molecules in aqueous salt solutions. In this paper, we use aqueous solutions of sodium iodide as a model system to study the influence of Förster energy transfer on the vibrational relaxation dynamics of anionic hydration shells.

[a]Electronic mail: lotze@amolf.nl

II. EXPERIMENTAL

We measure the vibrational relaxation dynamics of the OH stretch vibration of HDO and H_2O molecules for solutions of NaI in mixtures of H_2O/D_2O. The femtosecond pulses required for this study are generated by a series of nonlinear frequency conversion processes that are pumped with the pulses of a commercial Ti:sapphire regenerative amplifier (Spectra-Physics Hurricane). The amplifier system delivers 100 fs-pulses centered around 800 nm with a pulse energy of 0.8 mJ. About 500 μJ of the amplifier output is split off to pump a white-light seeded optical parametric amplifier (OPA, Spectra Physics) based on BBO (β-barium borate), generating signal and idler pulses with a wavelength around 1250 nm and 2200 nm, respectively. The idler pulses are frequency-doubled in a second BBO-crystal, and the resulting pulses at 1100 nm are used as a seed for parametric amplification in a $KTiOPO_4$-crystal (potassium titanyl phosphate) that is pumped by the remaining 300 μJ of 800 nm light, leading to amplification of the doubled idler and generation of mid-IR pulses at the difference frequency. The resulting mid-IR pulses have a wavelength of ~2.8 μm and have a duration of 180 fs, an energy of 5 μJ, and a spectral width of approximately 150 cm^{-1}.

We use the pulses in a pump-probe experiment. We generate probe and reference beams by splitting off a small portion (~4%) of the mid-IR light with a wedged CaF_2-window. The transmitted light is used as the pump beam. The probe is sent over a motorized delay stage to vary the time delay between the pump and probe pulses. The pump, probe, and reference are focused into the sample by a gold-coated off-axis parabolic mirror and recollimated by an identical mirror. The pump and probe foci are spatially overlapped in the sample. We measure the pump-induced transient absorption changes as a function of delay between the pump and the probe pulses. The reference is used for a pulse-to-pulse correction of the intensity fluctuations. The transmitted probe and reference beams are focused onto the entrance slit of a monochromator and frequency-dispersed on the two lines of a 2 × 32 mercury-cadmium-telluride (MCT) array. The pump beam is chopped at a frequency of 500 Hz to detect the pump-induced absorption changes. A variable λ/2-plate is used to set the polarization of the pump beam at 45° relative to that of the probe light. Behind the sample cell, a rotatable wire-grid polarizer is placed to select the polarization component of the probe beam parallel or perpendicular to the pump beam. From the parallel ($\Delta\alpha_{\parallel}$) and perpendicular ($\Delta\alpha_{\perp}$) components of the transient absorption changes, the isotropic signal is constructed:

$$\Delta\alpha_{iso}(\omega,t) = 1/3 \times \left(\Delta\alpha_{\parallel}(\omega,t) + 2 \times \Delta\alpha_{\perp}(\omega,t)\right). \quad (1)$$

We study aqueous solutions with NaI concentrations ranging from 1 to 6 mol/kg. NaI was purchased from Sigma Aldrich and used without further purification. The fraction of hydrogen

$$f_H = \frac{[H_2O]}{[H_2O] + [D_2O]} \quad (2)$$

was varied between 0.04 and 1 with $f_H = 1$ corresponding to neat H_2O. The samples were held between two CaF_2 windows separated by teflon spacers with thicknesses ranging from 3.8 to 25 μm. Samples containing neat H_2O were measured without spacer to avoid complete absorption of the infrared light due to the large absorption cross section of H_2O in the frequency region of the OH stretch vibration. The estimated length of these samples is 1 μm. We measured linear absorption spectra of the samples with a Perkin-Elmer spectrometer. In all experiments we tuned the center frequency of the mid-IR pulses to the maximum of the linear absorption spectrum.

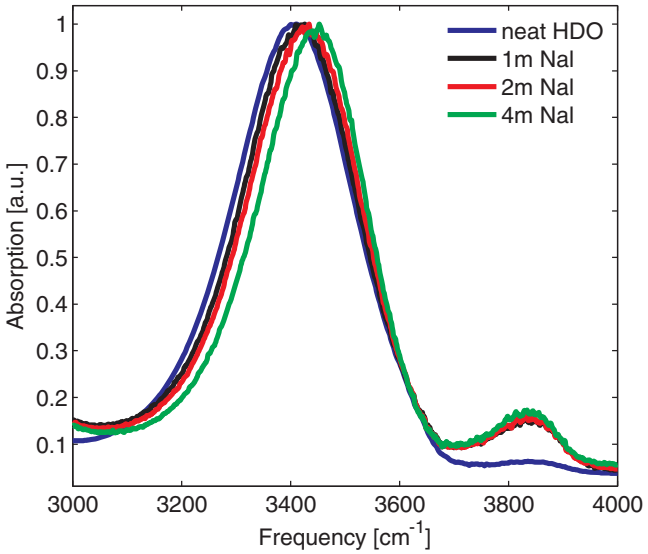

FIG. 1. Linear absorption spectra of the OH-stretching region for aqueous NaI solutions ($f_H = 0.04$) and neat HDO:D_2O.

III. RESULTS

A. Linear absorption spectra of HDO

Figure 1 shows linear absorption spectra in the OH stretch region for neat HDO:D_2O ($f_H = 0.04$) and for aqueous NaI solutions of the same isotopic composition with salt concentrations ranging from 1 mol/kg to 4 mol/kg. The OH stretch band is centered at 3400 cm^{-1} for neat HDO:D_2O, and shifts to higher frequencies upon the addition of NaI, an effect that has been observed before for aqueous solutions containing halide ions.[5,7,8,27] The blueshift results from the weakening of the hydrogen bonds upon the formation of anionic hydration shells. In particular, water molecules that donate a hydrogen bond to Cl^-, Br^-, or I^- ions absorb at a higher frequency than water molecules that donate a hydrogen bond to the oxygen atom of another water molecule. In the following, we will distinguish anion-bound and water-bound water molecules, the latter referring to water molecules for which both hydroxyl groups donate hydrogen bonds to the oxygen atoms of other water molecules.

B. Vibrational relaxation of water molecules in NaI solutions

Figure 2(a) shows transient absorption spectra that were measured for a 4m NaI solution ($f_H = 0.04$) at delay times ranging from 0.2 ps to 10 ps. The concentration of OH-groups

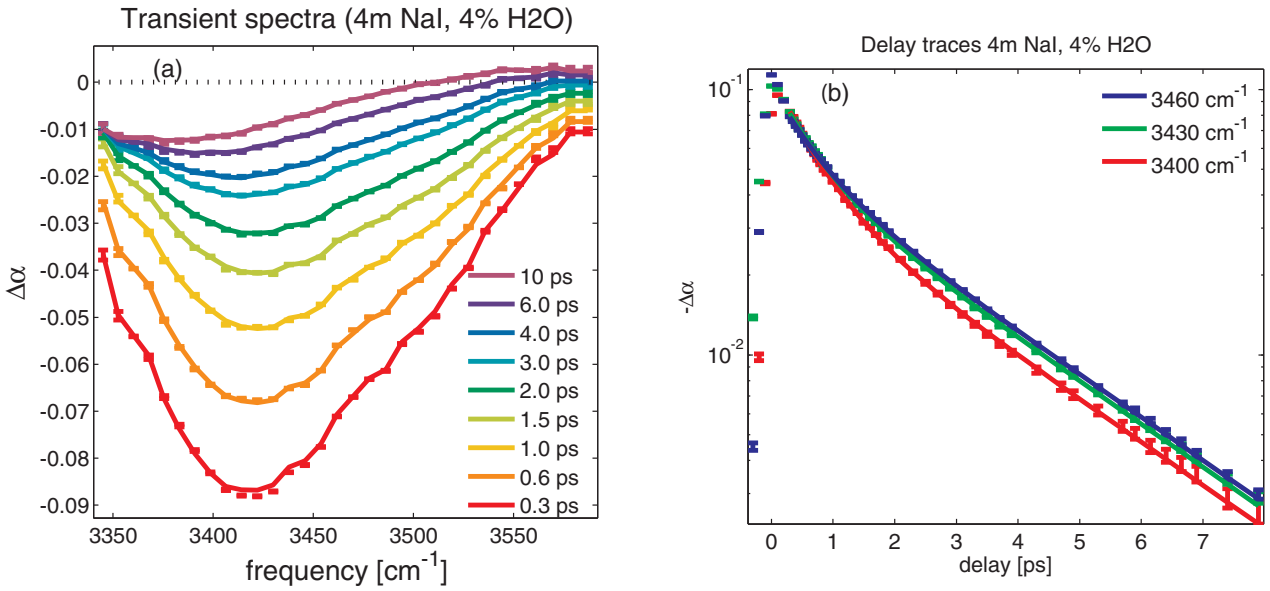

FIG. 2. (a) Transient spectra of a 4 mol/kg NaI solution ($f_H = 0.04$) at delay times of 0.3, 0.6, 1, 1.5, 2, 3, 4, 6, and 10 ps. (b) Heat-corrected delay traces of the same sample at frequencies of 3400, 3430, and 3460 cm^{-1}. The excitation frequency was centered at ~3430 cm^{-1}.

in this sample is sufficiently low to avoid Förster resonant energy transfer between the OH stretch vibrations.[24] Hence, this solution allows the study of the separate vibrational relaxation dynamics of anion-bound and water-bound water molecules. At early delay times, the spectra show a strong negative peak centered around 3420 cm^{-1}, originating from the bleaching of the ground state and stimulated emission from the first excited state. The excited state absorption ($1 \rightarrow 2$ transition) is red-shifted by 200 cm^{-1} from the fundamental transition and lies outside the spectral window of the experiment. At late delay times (>12 ps), the transient absorption spectra have the shape of a thermal difference spectrum, showing an induced absorption on the blue side and a bleaching-like signature in the red wing of the spectrum. This final spectrum results from the heating of the sample following the vibrational relaxation of the excited OH stretch vibration. This signal does not change over the time scale of the experiment (~1 ns).

The signal decays clearly faster on the red side of the spectrum than on the blue side. In Figure 2(b), we plot the transient absorption changes as a function of delay time at three different probe frequencies. The absorption changes have been corrected for the ingrowing heating signal. The signals are plotted on a logarithmic scale to show the strong non-exponential character of the decay. We observe a fast decay within the first two picoseconds, followed by a slower second decay process with a lifetime of several picoseconds. The amplitude of the slow component increases with frequency. We assign the fast component to water-bound HDO molecules showing a vibrational relaxation time constant of 740 fs.[28,29] The slow component is assigned to the OH groups of HDO molecules forming a hydrogen bond to the I^- anion.[8,9]

C. The influence of the H/D-ratio on the relaxation kinetics

To investigate how the relaxation dynamics depend on the isotopic composition of the sample, we varied the fraction of hydrogen f_H from 0.04 to 1. For a given f_H, the sample thickness was adjusted to give an absorbance of ~1 unit of optical density (OD) at the maximum of the OH-stretch absorption band. In Figure 3, we show a comparison between the transient absorption changes for different concentrations of NaI at an elevated H/D-ratio of $f_H = 0.2$. The decay curves in Fig. 3(b) have been corrected for the ingrowing heat signal. We observe a clear slow-down of the vibrational relaxation with increasing salt concentration, which can be understood from the increase of the fraction of iodide-bound HDO molecules.

Figure 4(a) shows that an increase of f_H leads to a rise of the final heat-signal relative to the magnitude of the initial bleach. This observation can be understood from the higher density of OH oscillators. For $f_H = 0.25$, 0.5, and 1, the energy of the pump-pulse that is absorbed by the sample is dumped in a smaller volume than in the case of $f_H = 0.04$, leading to a larger rise in temperature and thus to a higher heating signal. Figure 4(b) shows decay curves that have been corrected for the ingrowing heating signal and reveal the contribution to the decay curves that is due to vibrational relaxation only. A rise in the fraction of hydrogen in the sample clearly leads to an acceleration of the vibrational relaxation, ultimately leading to a nearly complete decay of the signal within 1.5 ps for $f_H = 1$ (dashed red curve). It is clear that neither of the two water components (water-bound and iodide-bound HDO) that were observed for $f_H = 0.04$ can be responsible for this fast decay. It is well known, however, that bulk H_2O-molecules have an extremely short vibrational lifetime of 200 fs.[25,30] Hence, we conclude that the presence of a significant fraction of H_2O-molecules at higher values of f_H opens up an additional, highly efficient vibrational relaxation channel. It is conceivable that the fast component in the decay curves is not only due to H_2O-molecules that are directly excited by the pump pulse, but also represents H_2O molecules that are excited by resonant energy transfer from the other water species in the sample. The other water species may thus employ

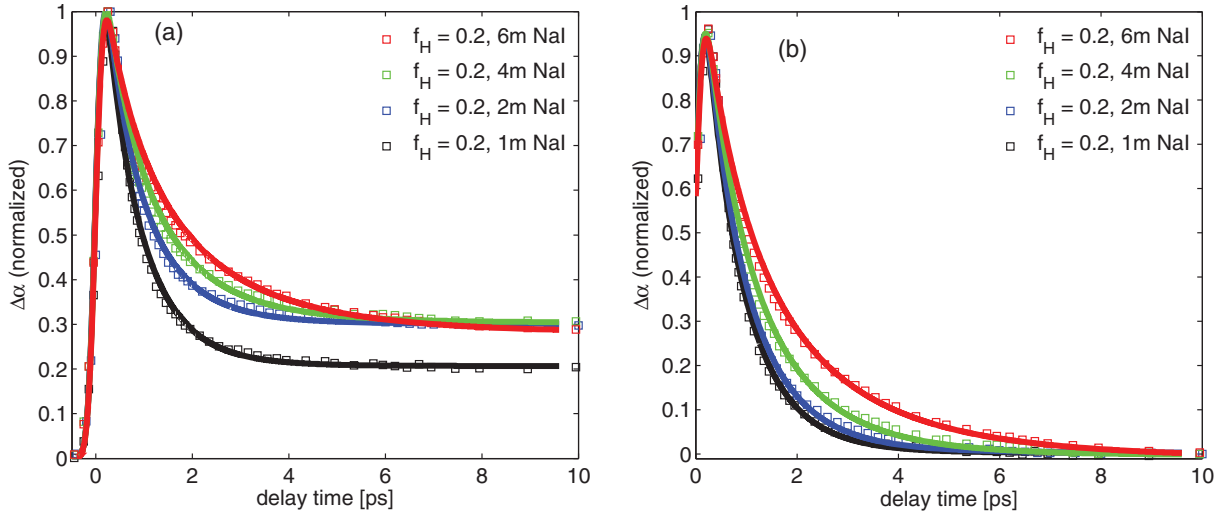

FIG. 3. (a) Transient absorption as a function of delay time for solutions containing 1, 2, 4, and 6m of NaI and a fraction of hydrogen $f_H = 0.2$. All signals are measured at a probe frequency of 3450 cm^{-1}. The excitation pulses were centered at frequencies between 3400 and 3450 cm^{-1}. The solid lines are obtained with the kinetic model described in the text. (b) The transient absorption changes (squares) together with the kinetic model (solid lines) after correction for the time-dependent grow-in of the heating signal. The vibrational relaxation slows down upon increasing the concentration of NaI.

near-by H_2O molecules as an efficient channel for vibrational relaxation.

D. Förster energy transfer

Förster energy transfer has been observed before for isotopic mixtures of neat water,[24,26] and leads to very efficient energy transfer among the hydroxyl stretch vibrations of the most abundant isotopic species. Förster energy transfer leads to a decay of the probability to find the excitation on the originally excited oscillator. Assuming a statistical distribution (radially and orientationally), Förster energy transfer leads to the following time-dependent survival probability of the excited oscillator:

$$S(t) = \exp\left(-\frac{4}{3} \times \pi^{3/2} \times C_{OH} \times \sqrt{R_0^6 \times t/T_1}\right), \qquad (3)$$

where C_{OH} denotes the number density of the OH-groups, R_0 is the Förster-radius, and T_1 is the pure vibrational relaxation time, unaffected by energy transfer. The term $\sqrt{R_0^6/T_1}$ represents the coupling between the donor and acceptor hydroxyl vibrations. The parameter T_1 enters in this expression to define the Förster radius R_0 as the distance between donor and acceptor for which energy transfer plays a role within the lifetime T_1. Hence, the value of the Förster-radius is referenced with respect to a T_1 value. Here, we define the Förster radius R_0 with respect to $T_1 = 200$ fs, the vibrational lifetime of the

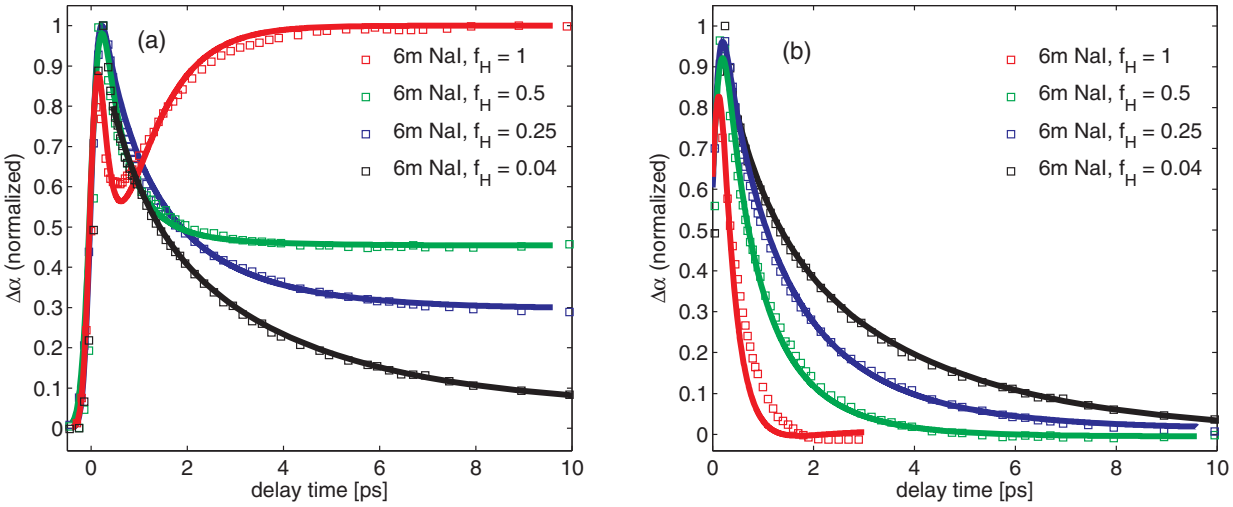

FIG. 4. (a) Transient absorption as a function of delay time for solutions with f_H varying from 0.04 (black squares) to 1 (red squares) and a NaI concentration of 6m. All signals are measured at a probe frequency of 3450 cm^{-1}. The excitation pulses were centered at a frequency of 3450 cm^{-1}. The solid lines are obtained with the kinetic model described in the text. (b) The transient absorption changes (squares) and the kinetic model (solid lines) after correction for the time-dependent grow-in of the heating signal. The vibrational relaxation accelerates upon increasing f_H.

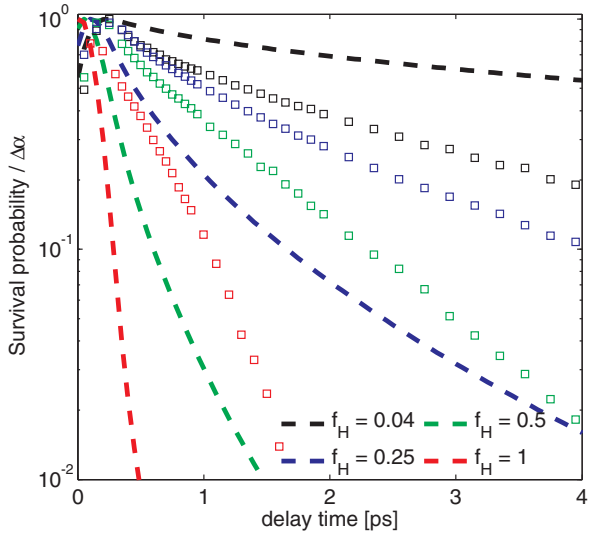

FIG. 5. Comparison of the decay of the survival probability according to Eq. (3) (dashed lines), reflecting the energy exchange, and the vibrational relaxation for different fraction of hydrogen, corrected for the grow-in of the heat signal (points). The concentration of NaI is 6 mol/kg for all curves. The vibrational relaxation curves have been normalized to unity for better comparison and the S(t)-curves have been convolved with a Gaussian of fwhm = 250 fs to include the effects of the duration of the laser pulses used in the experiment. Only in the isotopically most dilute sample ($f_H = 0.04$) the vibrational relaxation occurs faster than the exchange of energy.

O–H stretch vibrations of bulk H_2O. We keep this reference T_1 the same in fitting Eq. (3) to all studied solutions. As a result, the obtained values for R_0 are representative for the magnitudes of the average dipole-dipole couplings of the studied solutions. S(t) is the probability that an initially excited OH-group still remains excited after some time t, i.e., it represents the probability that the excitation has not yet hopped to another OH-group. It should be noted that the description of resonant energy transfer in terms of Eq. (3) also accounts for intramolecular energy transfer between OH-groups located on the same molecule, albeit in an approximate manner. Equation (3) is derived assuming a statistical distribution of OH oscillators (with a concentration of 111 M for pure H_2O) that starts at zero donor-accepter distance. Hence, intramolecular energy transfer is represented by the transfer between OH groups at typical mutual distances <2 Å. Obviously, this description is an approximation as the true intramolecular distance of the two O–H groups in the H_2O is not statistical.

In Figure 5, we show heat-corrected transient absorption changes for a 6m NaI solution with fractions of hydrogen of $f_H = 0.04, 0.25, 0.5, 1$. We compare these data with the decay of the survival probability according to Eq. (3). We use values of $T_1 = 200$ fs and $R_0 = 2.1$ A from Ref. 24 that were obtained from a pump-probe study on mixtures of HDO:D_2O. We calculate the number density of the accepting OH-oscillators from the given fraction of hydrogen via $C_{OH} = 2 \times f_H \times N_A \times \rho_{H_2O}/M_{H_2O}$, where N_A, ρ_{H_2O} and M_{H_2O} denote Avogadro's constant, the density of liquid H_2O, and the molar mass of H_2O, respectively.

Figure 5 shows that the decay of the survival probability is highly sensitive to the value of f_H. For $f_H = 0.04$, S(t) decays slowly over a time scale of several picoseconds. The comparison with the corresponding transient absorption changes reveals that the decay of the survival probability is slower than the vibrational relaxation, which implies that for $f_H = 0.04$ intermolecular coupling between the OH-groups of the water-bound or iodide-bound HDO-molecules is negligible. When increasing f_H to 0.25, the decay of the survival probability becomes strongly accelerated, leading to a drop to ~50% of its initial value within the first 500 fs. This finding implies that the excitation undergoes several "hopping" events from one OH-group to another before it relaxes. The effect of energy exchange on the relaxation dynamics is also notable when comparing the heat-corrected decay curves for different values of f_H (Figure 4(b)). The biexponential behavior that we observe for $f_H = 0.04$ is essentially absent for $f_H = 0.25$, 0.5, and 1. Instead we observe a quasi-monoexponential decay, indicative of an averaging of the lifetimes of different water species in the sample (water-bound HDO/H_2O, iodide-bound HDO/H_2O), a behavior that is caused by the exchange of excitation on a time scale shorter than the vibrational relaxation. We conclude that it is the rapid exchange of population that causes the speed-up of the vibrational relaxation, namely, by enabling the water-bound and anion-bound HDO-molecules to transfer their excitation to rapidly relaxing water-bound and anion-bound H_2O molecules.

E. Modeling the vibrational relaxation for all f_H

From Figures 4(b) and 5, it is obvious that the addition of hydrogen not only leads to an averaging, but also to a strong acceleration of the decay. We wish to establish a global model that is able to describe the experimentally obtained decay curves at any fraction of hydrogen and any concentration of NaI. To this purpose, we first need to determine the relative abundance of each of the different water species (anion-bound HDO/H_2O, water-bound HDO/H_2O). The amount of each water species in the sample can be quantified from only two parameters. The first parameter is the equilibrium constant K_{eq} of the isotope exchange reaction of water and heavy water:

$$H_2O + D_2O \leftrightarrow 2HDO \qquad (4)$$

that has been measured with NMR-spectroscopy.[31] From the equilibrium constant of this reaction, that is defined as

$$K_{eq} = [HDO]^2 / ([D_2O] \times [H_2O]) = 3.86 \qquad (5)$$

the amount of each of the three isotopomers in the sample at each f_H can be obtained. The second parameter required to determine the relative abundance of each water species is the hydration number of the iodide ion. We obtain this hydration number from a description that was used in Ref. 9 that accounts for the presence of unoccupied sites in the hydration shell of the iodide ion.

$$K_{iodide} = [OH \cdots I] / ([I_S] \times [OH \cdots O]), \qquad (6)$$

where $[I_s]$ denotes the concentration of unoccupied sites in the ion's hydration shell. When the association constant K_{iodide} and the maximum number of water molecules in the first hydration shell are known, the fraction of anion-bound

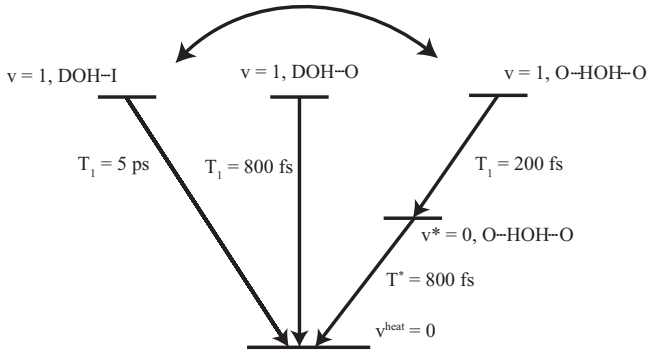

FIG. 6. The kinetic model used to fit the experimental data for $f_H = 0.15$, 0.2, 0.25, 0.5, and 1, and NaI concentrations of 1, 2, 4, and 6m. The time-dependent Förster-rate $k_F(t)$ is calculated as outlined in the text. The vibrational T_1 relaxation time constants are obtained from the literature.

and water-bound OH-groups can be calculated at any concentration of NaI. We use a value for K_{iodide} of 0.25 as used in Ref. 9, and assume a maximum number of 8 water molecules to reside in the hydration shell of the I^- ion. Hence, $[OH\cdots I]+[I_s] = 8*[I^-]$. Equations (5) and (6) are used to calculate the amount of water-bound HDO, anion-bound HDO, water-bound H_2O, and anion-bound H_2O. The kinetic model that we employ to describe the experimentally observed relaxation dynamics is illustrated in Figure 6. We assume the presence of three excited states, namely, water-bound and anion-bound HDO and H_2O (bound to water or to the anion) molecules that have different intrinsic vibrational lifetimes. Each of the three species is allowed to exchange energy with each of the other species via Förster-energy transfer. By differentiation of Eq. (3), one obtains the following expression for the time-dependent Förster-rate k_F:

$$k_F(t) = \frac{2}{3} \times \pi^{3/2} \times C_{OH} \times \sqrt{R_0^6/T_1} \times t^{-1/2} \qquad (7)$$

with $T_1 = 200$ fs and the number density of accepting OH-groups C_{OH} being calculated as outlined in Sec. III D. The coupled rate-equations are outlined in the Appendix and numerically solved by a 4th-order Runge-Kutta algorithm, including the cross-correlate of the pump and probe pulses. The vibrational lifetimes of all three excited states are available from previous studies.[8,28,30] Following previous studies on the vibrational relaxation of bulk H_2O,[25,30] we include an intermediate state in the relaxation of H_2O with a lifetime of 800 fs that accounts for delayed grow-in of the heat signal. The intrinsic vibrational lifetime of the O–H groups of H_2O molecules that donate one or two hydrogen bonds to I^- ions is not known, as the vibrational relaxation of these species will always be dominated by intramolecular energy transfer and/or energy transfer to the very fast relaxing H_2O molecules that show a T_1 of 200 fs. However, the rapid initial decay of the signal for $f_H = 1$ of Fig. 4(a) shows that the intrinsic T_1 time constant of iodide-bound H_2O molecules must be fast and close to 200 fs. If the T_1 of iodide-bound H_2O would have been significantly longer than 200 fs, the initial decay would have slowed down with increasing iodide concentration, because the initial decay represents the averaged vibrational relaxation of bulk-like and iodide-bound H_2O molecules. We observe a similar rapid initial decay at all studied NaI concentrations and $f_H = 1$. Therefore, in modelling the data we take the intrinsic relaxation behaviour of the I^- bonded H_2O molecules to be the same as for bulk H_2O molecules.

We perform a fit of 20 experimental datasets with a model that employs only a single adjustable parameter, namely, the Förster-radius R_0. Figures 3(a) and 4(a) show that the fitted curves are in excellent agreement with the experimental data at all salt concentrations and all fractions of hydrogen. We find the Förster-radius R_0 to depend slightly on the concentration of sodium iodide, having values of 2.5 ± 0.2 Å at 1m and 2m NaI, 2.4 ± 0.2 Å at 4m NaI, and 2 ± 0.2 Å at 6m NaI. For comparison, the Förster-radius of neat H_2O was found to be 2.1 Å.[24]

IV. DISCUSSION

We observe that an increase in the fraction of hydrogen leads to an acceleration of the vibrational relaxation of *all* water OH vibrations present in aqueous solutions of NaI. This acceleration of all water OH groups can be explained from the rapid resonant energy transfer between the different water species. For water hydroxyl groups with an intrinsically slow relaxation such as the OH groups of HDO molecules donating a hydrogen bond to I^-, the resonant energy transfer to H_2O opens up an additional efficient relaxation channel. The comparably long relaxation time of the HDO molecules donating a hydrogen bond to I^- has been explained in terms of a reduced anharmonic coupling between the excited OH stretch vibration and the $OH\cdots I^-$ hydrogen-bonding mode.[8] The fast decay of the stretch band of H_2O molecules has been explained by the Fermi-resonance of the OH stretch vibrations with the overtone of the bending mode.[30,32]

In Fig. 4(b), it is seen that the fitted curve for $f_H = 1$ (solid red line, representing the convolution of the cross-correlate and the vibrational relaxation with $T_1 = 200$ fs) deviates from the heat-corrected data points at later delay times. This deviation may originate from the description of the rise of the thermal signal with a single (exponential) time constant. It is conceivable that at salt concentrations as high as 6 mol/kg this assumption is not fully appropriate anymore and that the dynamics of the heat grow-in are heterogeneous in nature and would thus be given by a distribution of rates rather than a single time constant.

Our modeling of the resonant energy transfer in terms of the survival probability (Eq. (3)) is based on the assumption of a randomly oriented distribution of acceptor molecules. Furthermore, we assume that the transfer of the vibrational excitation occurs irreversibly. The assumption of a statistical distribution is of course a simplification of the actual physical picture. The validity of these assumptions has been studied in a recent paper by the Skinner group.[33] In this study, it was found that the effects of the reversibility of the energy transfer and the influence of the relative orientation and spatial distribution of the OH oscillators on the rate of resonant energy transfer counteract each other to some extent, making Eq. (3) a reasonable approximation to describe the dynamics of Förster energy transfer in liquid water.

The rate of resonant energy transfer between different types of oscillators depends on the overlap of the homogeneous lineshapes and the cross sections.[34] The rate of energy transfer from iodide-bound to water-bound water molecules can thus differ from the rate of energy transfer between bulk water molecules. For the iodide bound water, the absorption band is narrower and the cross-section is somewhat larger, leading to an increase of the resonant energy transfer rate. On the other hand, the central frequencies of the OH · · · I and OH · · · O vibrations differ, leading to a decrease of the rate of energy transfer. It is to be expected that these effects more or less compensate each other, thus explaining why the fitted Förster-radius does not change dramatically with increasing NaI concentration. The small decrease of the Förster-radius from 2.5 ± 0.2 Å at 1m to 2 ± 0.2 Å at 6m NaI most likely results from a dilution effect: the Na^+ and I^- ions take up space, thereby increasing the average distance between the hydroxyl groups of the water molecules.

V. CONCLUSIONS

We measured the vibrational relaxation dynamics of the OH-stretch vibration in aqueous solutions of sodium iodide of different isotopic composition. For low fractions of hydrogen ($f_H = 0.04$), we observe two separately decaying water species that we assign to water-bound and iodide-bound HDO molecules. Increasing the hydrogen fraction leads to a drastic change in the relaxation behavior. We observe fast Förster-energy transfer of the vibrational excitation between the different water species present in the sample, i.e., the ion hydration shell and the bulk water. For HDO molecules in the hydration shell of the anion the resonant energy transfer to H_2O molecules opens up a new vibrational relaxation channel that is much faster than the intrinsic vibrational relaxation. Hence, the resonant energy transfer strongly accelerates the vibrational energy relaxation of the anionic hydration shells. For $f_H \geq 0.25$, the Förster energy transfer is faster than the intrinsic vibrational relaxation rates of all the water species, and a single decay rate is observed that forms a weighted average of the relaxation rates of the different species. We model the data with a kinetic model that includes the Förster energy transfer between the different water species. This model provides an excellent description of the data for all studied NaI concentrations and isotope compositions. From the model we find that the Förster radius decreases from 2.5 ± 0.2 Å at 1m NaI to 2 ± 0.2 Å at 6m NaI. This means that the Förster energy transfer becomes somewhat slower at higher salt concentrations, most probably because the average distance between the water molecules increases as a result of the dilution of water due to the presence of Na^+ and I^- ions.

ACKNOWLEDGMENTS

This work is part of the research program of the Stichting voor Fundamenteel Onderzoek der Materie (FOM), which is financially supported by the Nederlandse Organisatie voor Wetenschappelijk Onderzoek (NWO). The authors would like to thank Nuria Garcia-Araez for experimental support.

APPENDIX: ■

The coupled rate-equations for the relaxation scheme outlined in Figure 6 read as follows:

$$\frac{d\,[\mathrm{DOH}\cdots\mathrm{I}]}{dt} = -\frac{1}{T_1^{\mathrm{DOH}\cdots\mathrm{I}}}\,[\mathrm{DOH}\cdots\mathrm{I}] - k_F(t)\,[\mathrm{DOH}\cdots\mathrm{I}] + k_F(t)\;f_{\mathrm{DOH}\cdots\mathrm{I}}([\mathrm{DOH}\cdots\mathrm{O}] + [\mathrm{DOH}\cdots\mathrm{I}] + [\mathrm{HOH}]), \tag{A1}$$

$$\frac{d\,[\mathrm{DOH}\cdots\mathrm{O}]}{dt} = -\frac{1}{T_1^{\mathrm{DOH}\cdots\mathrm{O}}}\,[\mathrm{DOH}\cdots\mathrm{O}] - k_F(t)\,[\mathrm{DOH}\cdots\mathrm{O}] + k_F(t)\,f_{\mathrm{DOH}\cdots\mathrm{O}} \times ([\mathrm{DOH}\cdots\mathrm{O}] + [\mathrm{DOH}\cdots\mathrm{I}] + [\mathrm{HOH}]), \tag{A2}$$

$$\frac{d\,[\mathrm{HOH}]}{dt} = -\frac{1}{T_1^{\mathrm{HOH}}}\,[\mathrm{HOH}] - k_F(t)\,[\mathrm{HOH}] + k_F(t)\,f_{\mathrm{HOH}}([\mathrm{DOH}\cdots\mathrm{O}] + [\mathrm{DOH}\cdots\mathrm{I}] + [\mathrm{HOH}]), \tag{A3}$$

$$\frac{d\left[\mathrm{HOH}^*\right]}{dt} = \frac{1}{T_1^{\mathrm{HOH}}}\,[\mathrm{HOH}] - \frac{1}{T_1^*}\left[\mathrm{HOH}^*\right], \tag{A4}$$

$$\frac{d[v^{heat}=0]}{dt} = \frac{1}{T_1^*}\left[\mathrm{HOH}^*\right] + \frac{1}{T_1^{\mathrm{DOH}\cdots\mathrm{I}}}\,[\mathrm{DOH}\cdots\mathrm{I}] + \frac{1}{T_1^{\mathrm{DOH}\cdots\mathrm{O}}}\,[\mathrm{DOH}\cdots\mathrm{O}]\,. \tag{A5}$$

Each of the three excited states [DOH· · ·I], [DOH· · ·O], and [HOH] decays with its respective T_1-lifetime. We have used values of $T_1^{\mathrm{DOH}\cdots\mathrm{I}} = 5$ ps, $T_1^{\mathrm{DOH}\cdots\mathrm{O}} = 800$ fs, $T_1^{\mathrm{O}\cdots\mathrm{HOH}\cdots\mathrm{O}} = 200$ fs, and $T^* = 800$ fs.[8,28,30] In addition, each excited state transfers population to the other two excited states via Förster-energy transfer, which is described by the second term in Eqs. (A1)–(A3). The time-dependent Förster-rate $k_f(t)$ is calculated according to Eq. (7). At the same time, each state gains population from the other excited states according to its relative abundance in the sample. The back transfer is accounted for by the last term in Eqs. (A1)–(A3). The relative weighting factors f_i in Eqs. (A1)–(A3) are calculated from Eqs. (5) and (6). Numerical integration of the above rate equations is performed with a 4th-order Runge-Kutta algorithm and yields the population of all involved states at every time point t.

We have introduced a scaling factor of 2.5 for the contribution of H_2O molecules at all salt concentration and fractions of hydrogen to account for the larger absorption cross-section of this species in comparison to water-bound and iodide-bound HDO.

[1] R. D. Waldron, J. Chem. Phys. **26**(4), 809–814 (1957).
[2] W. M. Cox and J. H. Wolfenden, Proc. R. Soc. London, Ser. A **145**(855), 475–488 (1934).

[3]Y. Marcus, Chem. Rev. **109**(3), 1346–1370 (2009).
[4]K. J. Tielrooij, N. Garcia-Araez, M. Bonn, and H. J. Bakker, Science **328**(5981), 1006–1009 (2010).
[5]M. D. Fayer, D. E. Moilanen, D. Wong, D. E. Rosenfeld, E. E. Fenn, and S. Park, Acc. Chem. Res. **42**(9), 1210–1219 (2009).
[6]D. E. Moilanen, D. Wong, D. E. Rosenfeld, E. E. Fenn, and M. D. Fayer, Proc. Natl. Acad. Sci. U.S.A. **106**(2), 375–380 (2008).
[7]S. Park and M. D. Fayer, Proc. Natl. Acad. Sci. U.S.A. **104**(43), 16731–16738 (2007).
[8]M. F. Kropman and H. J. Bakker, J. Chem. Phys. **115**(19), 8942–8948 (2001).
[9]M. F. Kropman and H. J. Bakker, J. Am. Chem. Soc. **126**(29), 9135–9141 (2004).
[10]M. F. Kropman and H. J. Bakker, Science **291**(5511), 2118–2120 (2001).
[11]M. F. Kropman, H. K. Nienhuys, and H. J. Bakker, Phys. Rev. Lett. **88**(7), 077601 (2002).
[12]A. W. Omta, M. F. Kropman, S. Woutersen, and H. J. Bakker, Science **301**(5631), 347–349 (2003).
[13]J. B. Asbury, T. Steinel, C. Stromberg, S. A. Corcelli, C. P. Lawrence, J. L. Skinner, and M. D. Fayer, J. Phys. Chem. A **108**(7), 1107–1119 (2004).
[14]R. L. A. Timmer and H. J. Bakker, J. Phys. Chem. A **113**(21), 6104–6110 (2009).
[15]M. Ji, M. Odelius, and K. J. Gaffney, Science **328**(5981), 1003–1005 (2010).
[16]D. Laage and J. T. Hynes, Proc. Natl. Acad. Sci. U.S.A. **104**(27), 11167–11172 (2007).
[17]A. M. Dokter, S. Woutersen, and H. J. Bakker, Proc. Natl. Acad. Sci. U.S.A. **103**(42), 15355–15358 (2006).
[18]I. R. Piletic, D. E. Moilanen, D. B. Spry, N. E. Levinger, and M. D. Fayer, J. Phys. Chem. A **110**(15), 4985–4999 (2006).
[19]D. Laage and J. T. Hynes, Science **311**(5762), 832–835 (2006).
[20]C. J. Fecko, J. J. Loparo, S. T. Roberts, and A. Tokmakoff, J. Chem. Phys. **122**(5), 054506–054518 (2005).
[21]J. Stenger, D. Madsen, P. Hamm, E. T. J. Nibbering, and T. Elsaesser, J. Phys. Chem. A **106**(10), 2341–2350 (2002).
[22]J. B. Asbury, T. Steinel, K. Kwak, S. A. Corcelli, C. P. Lawrence, J. L. Skinner, and M. D. Fayer, J. Chem. Phys. **121**(24), 12431–12446 (2004).
[23]T. Steinel, J. B. Asbury, J. Zheng, and M. D. Fayer, J. Phys. Chem. A **108**(50), 10957–10964 (2004).
[24]S. Woutersen and H. J. Bakker, Nature (London) **402**(6761), 507–509 (1999).
[25]M. L. Cowan, B. D. Bruner, N. Huse, J. R. Dwyer, B. Chugh, E. T. J. Nibbering, T. Elsaesser, and R. J. D. Miller, Nature (London) **434**(7030), 199–202 (2005).
[26]L. Piatkowski, K. B. Eisenthal, and H. J. Bakker, Phys. Chem. Chem. Phys. **11**(40), 9033–9038 (2009).
[27]P. A. Bergstroem, J. Lindgren, and O. Kristiansson, J. Phys. Chem. **95**(22), 8575–8580 (1991).
[28]Y. L. A. Rezus and H. J. Bakker, J. Chem. Phys. **125**(14), 144512–144519 (2006).
[29]S. Woutersen, U. Emmerichs, H.-K. Nienhuys, and H. J. Bakker, Phys. Rev. Lett. **81**(5), 1106–1109 (1998).
[30]A. J. Lock and H. J. Bakker, J. Chem. Phys. **117**(4), 1708–1713 (2002).
[31]J. C. Duplan, L. Mahi, and J. L. Brunet, Chem. Phys. Lett. **413**(4–6), 400–403 (2005).
[32]S. Ashihara, N. Huse, A. Espagne, E. T. J. Nibbering, and T. Elsaesser, Chem. Phys. Lett. **424**(1–3), 66–70 (2006).
[33]M. Yang, F. Li, and J. L. Skinner, J. Chem. Phys. **135**(16), 164505–164510 (2011).
[34]T. Förster, Ann. Phys. **437**(1–2), 55–75 (1948).